# Supporting Information

## Levental et al. 10.1073/pnas.1016184107

### SI Methods.

**Cell Culture and Treatment.** Rat basophilic leukemia (RBL) cells were cultured in medium containing 60% MEM, 30% RPMI medium 1640, and 10% FCS supplemented with 2 mM glutamine, 100 U/mL penicillin, and 100 μg/mL streptomycin at 37 °C in humidified 5% $CO_2$. For palmitoylation inhibition, cells were washed 2 times, then preincubated for 10 min in incubation medium (MEM + 2.5% FCS + 0.25% fatty acid-free bovine serum albumin), and then treated with 100 μM 2-bromopalmitate in incubation medium for 3 h at 37 °C.

**Giant Plasma Membrane Vesicle (GPMV) Labeling and Treatment.** GPMVs were labeled by adding fluorescently modified lipids or proteins directly to the GPMV suspension for 30 min at 4 °C. The labels used were (final concentrations in parentheses): 1,2-dioleoyl-sn-glycero-3-phosphoethanolamine-N-lissamine rhodamine B sulfonyl (rhPE; Avanti Polar Lipids; 1 μg/mL); cholera toxin B subunit Alexa 488 (CTxB; MoBiTec; 2 μg/mL); Alexa-488 Proaerolysin (FLAER; Pinewood Scientific Services; 0.01 μM). Vesicles were imaged under temperature controlled conditions (at 5 °C) as described (1). For postisolation treatments in Fig. 2, vesicles were incubated with DTT (2 mM or 20 mM), paraformaldehyde (25 mM), and/or *N*-ethylmaleimide (NEM) (2 mM) for 1 h at 37 °C. For total protein quantification in Fig. 4, DTT treatment was 20 mM for 1 h at 37 °C and GPI-specific phospholipase (PI-PLC) was 0.1 U/mL for 15 min at 4 °C.

**Plasmids and Transfection.** Plasmids used in this study were linker for activation of Tcells (LAT)-GFP, LAT-transmembrane domain (TMD)-GFP, and GPI-GFP described in ref. 2, LAT-TMD-mRFP (monomeric Red Fluorescent Protein) in ref. 3, and LAT-IDer (Inducible Dimer) in ref. 4. H-ras-GFP, transferrin receptor (TfR)-GFP, and Sec61-GFP were obtained as generous gifts from Dr. Anne Kenworthy (Vanderbilt University, Nashville, TN), Dr. Lawrence Rajendran (Swiss Federal Institute of Technology, Zurich, Switzerland), and Dr. Nica Borgese (University of Milan, Milan, Italy), respectively. The C26 and C29 mutants of trLAT were generated using the QuickChange site-directed mutagenesis kit (Stratagene) using the supplied protocol. Transfection was done using the AMAXA Nucleofection kit (Lonza) using the supplied protocol.

In the LAT-IDer experiments, addition of the IDer tag induced a slight perturbation in raft phase partitioning in nGPMVs, leading to a modest depletion of trLAT-IDer from the raft phase (Fig. 3 *A*, *Left*, and *B*). Treatment of the GPMVs postisolation with the dimerizing agent AP20187 (Ariad; 0.5 μM as in ref. 4) reversed phase partitioning and induced strong raft phase enrichment.

**Acyl-Biotinyl Exchange.** Acyl-biotinyl exchange to quantify the relative amount of palmitoylation in the DTT treated samples was performed essentially as described (5) with the optional membrane purification steps (2 and 3 in the reference) included. Briefly, membranes were prepared from RBL cells without lysis, followed by detergent solubilization and treatment with either DTT (2 or 20 mM) or hydroxylamine (HAM) (0.5 M). The protein solutions were then treated with 10 mM NEM to block all free thiol groups (unpalmitoylated cysteines). Next, 0.7 M HAM was used to specifically remove S-linked fatty acids, and the newly exposed cysteines were concomitantly labeled with a thiol-reactive biotin reagent (N-[6-(Biotinamido)hexyl]-3′-(2′-pyridyldithio)propionamide). The biotinylated (formerly palmitoylated) proteins were then pulled down using streptavidin-agarose. Protein solutions were chloroform/methanol precipitated three times between each step, as described (5). Subsequent silver staining and Western blotting of the eluted proteins was done according to standard protocols using a goat polyclonal antibody against LAT (sc-5321; Santa Cruz Biotec).

**Labeling of Total Extracellular Proteins and Quantification Details.** Cells were labeled with membrane-impermeable, amine-reactive biotin to nonspecifically biotinylate all surface-exposed proteins. Cells were washed 3× in PBS, then incubated on ice for 30 min in the presence of Sulfo-NHS-biotin (1 mg/mL; Sigma). The reaction was quenched by washing the cells twice with 0.1 mM glycine, then incubating for 5 min on ice. GPMVs were produced and stained with binding cholera toxin (CTxB) as above then counterstained with a monomeric Fab fragment of goat anti-biotin coupled to Texas Red (1 μg/mL; Rockland Immunochemicals).

Images of the Texas Red signal were quantified as above to derive $K_{p,\mathrm{raft}}$ (Fig. S2), which was then used to calculate the percentage of signal in the CTxB-rich (raft) phase in each vesicle by

$$x_{\mathrm{raft}} = \frac{K_{p,\mathrm{raft}}}{1 + K_{p,\mathrm{raft}}},$$

which was taken to be equivalent to the fraction of biotinylation-accessible (i.e., cell surface exposed) protein in the raft phase. For this calculation to be valid, the relative abundance of the two phases must be equal, which was validated by measuring the relative surface area of the spherical caps as in ref. 1 (measured abundance of raft phase = 56 ± 13%). Correlating protein amount to fluorescence signal requires that the fluorescent yield from the antibody-coupled fluorophore is equivalent in the two phases, which we believe is very likely, considering the fluorophore is located very far from the membrane environment (external proteins coupled with biotin to which the labeled antibody fragment is bound).

GPMVs were treated with 20 mM DTT as above to remove all S-linked fatty acids (Fig. 5*A*). This treatment led to a large reduction in relative raft phase fluorescence, which was taken as evidence of depalmitoylation-induced nonraft missorting of acylated TM proteins (as these are the only proteins known to be both S-acylated and accessible to external labeling). According to this assumption, loss of raft phase signal would lead to an increase in nonraft phase signal (proteins repartitioning from raft to nonraft instead of being lost from the membrane); therefore, the fraction of proteins lost from the raft phase is calculated by

$$F_{\mathrm{palm}} = x_{\mathrm{raft,ctrl}} - x_{\mathrm{raft,DTT}},$$

where $F_{\mathrm{raft,palm}}$ is the fraction of protein whose raft residence depends on DTT-sensitive palmitoylation, and $x_{\mathrm{raft,ctrl}}$ and $x_{\mathrm{raft,DTT}}$ are the measured fractions of protein in the raft phase before and after DTT treatment, respectively (Fig. 5*C*).

A similar calculation was performed for PI-PLC treated (0.1 U/mL) GPMVs. We showed that this treatment reduced GPI-APs in RBL nGPMVs by 90% (Fig. S3). An important difference in this case is that signal lost from the raft phase (through hydrolysis of the GPI anchor) is not gained by the nonraft phase and instead lost to the medium. Therefore the calculation differs slightly in that it is important to take into account the relative partitioning of GPI-anchored proteins (APs) between phases.

We have assumed the fraction of raft resident GPI-APs ($x_{\text{raft,GPI-AP}}$) to be 0.8 by averaging data from three different sources: our own measurements of GPI-GFP partitioning in GPMVs ($x_{\text{raft,GPI-AP}} = 0.78$) and image analysis of two different published image sets of GPI-AP partitioning in GPMVs—Sengupta et al. (6) (GPI-GL-GFP; $x_{\text{raft,GPI-AP}} = 0.83$) and Baumgart et al. (7) (Thy-1 ; $x_{\text{raft,GPI-AP}} = 0.79$). The good quantitative agreement between these completely independent measurements gives us confidence that this is a reasonable estimate of GPI-AP partitioning in GPMVs. Using these data, the calculation for GPI-AP raft resident proteins is

$$\frac{x_{\text{ctrl}} - x_{\text{raft,GPI-AP}} * E_{\text{PI-PLC}} * F_{\text{GPI-AP}}}{(1 - x_{\text{ctrl}}) - (1 - x_{\text{raft,GPI-AP}}) * E_{\text{PI-PLC}} * F_{\text{GPI-AP}}} = K_{p,\text{raft,PI-PLC}},$$

where $F_{\text{GPI-AP}}$ is the fraction of labeled proteins that are GPI-APs, $E_{\text{PI-PLC}}$ is the efficiency of PI-PLC hydrolysis of GPI-APs (measured to be 90%—Fig. S3), and $K_{p,\text{raft,PI-PLC}}$ is the partition coefficient of the total external protein after PI-PLC treatment (Fig. S2). The fraction or protein whose raft residence is due to their GPI anchor is then

$$F_{\text{raft,GPI-AP}} = F_{\text{GPI-AP}} * x_{\text{raft,GPI-AP}}.$$

**Detergent Resistance of trLAT-IDER.** Detergent resistant membranes (DRMs) were isolated essentially as described (8). Briefly, transfected cells were washed twice with ice cold TNE (50 mM Tris-HCl, 150 mM NaCl, 2 mM EDTA, pH 7.4) then scraped and centrifuged at 500 × *g* for 10 min. The pellet was resuspended in TNE supplemented with protease inhibitor cocktail and the cells were homogenized by passing through a G25 needle 15 times. The homogenate was then solubilized in 1% TX-100 (Pierce) on ice for 30 min. The sample was then bottom-loaded into a 3-step iodixanol gradient (1.2 mL of 40%, 2.1 mL of 30%, 0.9 mL of 5%) and centrifuged at 40,000 rpm for 4 h at 4 °C. Six fractions of 700 μL were then taken from the top and Western blotted for specific markers.


1. Levental I, et al. (2009) Cholesterol-dependent phase separation in cell-derived giant plasma-membrane vesicles. *Biochem J* 424:163–167.
2. Meder D, Moreno MJ, Verkade P, Vaz WL, Simons K (2006) Phase coexistence and connectivity in the apical membrane of polarized epithelial cells. *Proc Natl Acad Sci USA* 103:329–334.
3. Lingwood D, Ries J, Schwille P, Simons K. (2008) Plasma membranes are poised for activation of raft phase coalescence at physiological temperature. *Proc Natl Acad Sci USA* 105:10005–10010.
4. Lingwood D, Schuck S, Ferguson C, Gerl MJ, Simons K (2009) Generation of cubic membranes by controlled homotypic interaction of membrane proteins in the endoplasmic reticulum. *J Biol Chem* 284:12041–12048.
5. Wan J, Roth AF, Bailey AO, Davis, NG (2007) Palmitoylated proteins: Purification and identification. *Nat Protoc* 2:1573–1584.
6. Sengupta P, Hammond A, Holowka D, Baird B (2008) Structural determinants for partitioning of lipids and proteins between coexisting fluid phases in giant plasma membrane vesicles. *BBA—Biomembranes* 1778:20.
7. Baumgart T, et al. (2007) Large-scale fluid/fluid phase separation of proteins and lipids in giant plasma membrane vesicles. *Proc Natl Acad Sci USA* 104:3165–3170.
8. Lingwood D, Simons K (2007) Detergent resistance as a tool in membrane research. *Nat Protoc* 2:2159–2165.


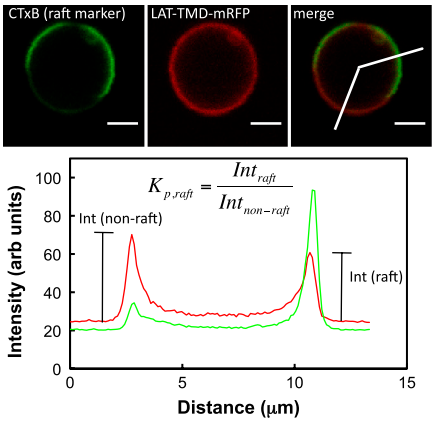


**Fig. S1.** *Fluorescent quantification of $K_{p,\text{raft}}$.* Partition coefficients for GPMV components are quantified by line scans through the two domains and dividing the intensities. Only vesicles with clearly defined equatorial domains (as shown) were used for partitioning quantification. Shown is a pdGPMV with LAT-TMDmRFP stained with the raft marker CTxB. Vesicles shown in all figures are 5–10 μm diameter.

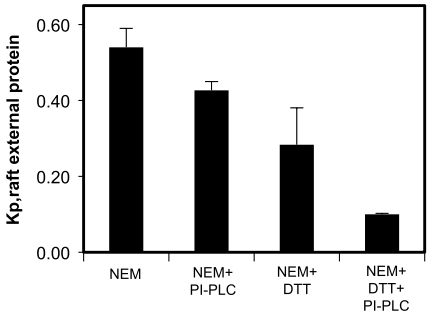


**Fig. S2.** *Raft partitioning of total protein is a function of DTT and PI-PLC treatments.* Partition coefficients for GPMV components are quantified by line scans through the two domains and dividing the intensities, as described in detail below. Error bars are average + SD from three independent experiments, each with 10–15 vesicles per condition.

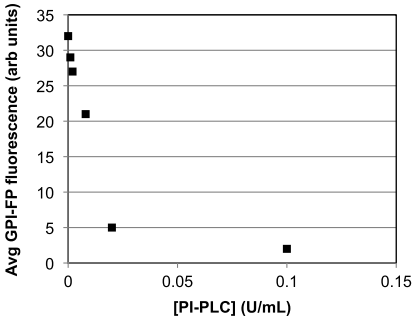


**Fig. S3.** *PI-PLC eliminates 90% of surface GPI-APs*. (*A*) PI-PLC activity evaluated by removal of GPI-GFP fluorescence from GPMVs. GPMVs isolated from GPI-GFP transfected cells were treated postisolation with the indicated concentrations of PI-PLC and the average fluorescence was measured from >30 vesicles/condition. (*B*) FLAER (a fluorescently conjugated bacterial GPI-binding toxin) binding is reduced by 90% when GPMVs are treated with 0.1 U/mL PI-PLC. This result confirms that nearly all GPI-APs on the surface of RBLs are PI-PLC sensitive.

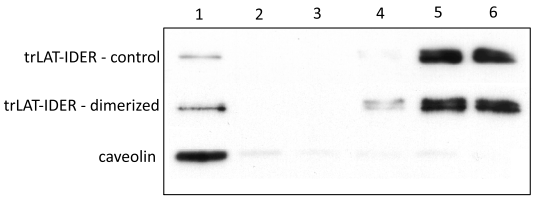


**Fig. S4.** *Detergent resistance of trLAT-IDER is enhanced by dimerization*. trLAT-IDER is somewhat resistant to TX100 solubilization at 4 °C as evidenced by its presence in the caveolin-rich, low-density fraction of a density gradient. Induced dimerization enhances this affinity for DRMs, correlating with the increased raft phase partitioning observed under these conditions.

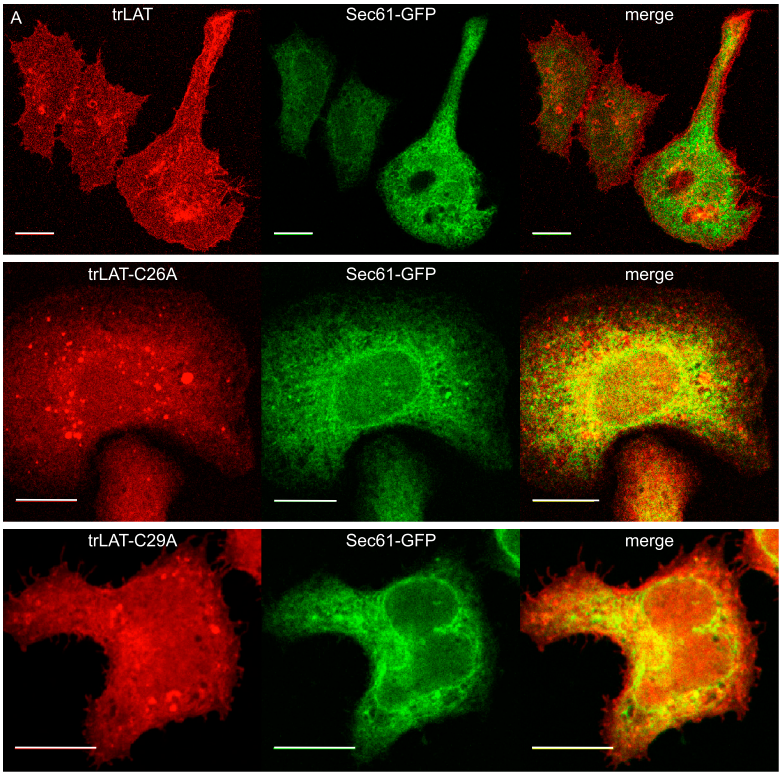


**Fig. S5.** *Trafficking of trLAT correlates with raft partitioning*. While the wild-type trLAT is localized at the plasma membrane, the C26A mutant is somewhat arrested in the endoplasmic reticulum (as judged by colocalization with the ER marker Sec61-GFP), with an intermediate phenotype observed for trLAT-C29A. Scale bars are 10 μm.

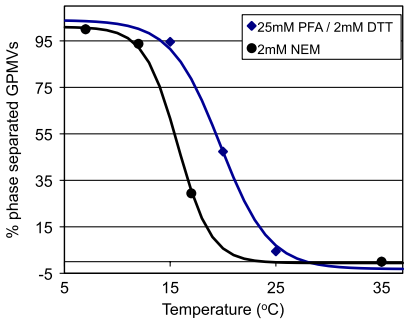


**Fig. S6.** *Effect of isolation agent on GPMV phase separation*. Phase separation behavior was notably different between nGPMVs and pdGPMVs, with the phase transition temperature 5–10 °C higher in pdGPMVs, requiring significant cooling of nGPMVs before phase separation was observed. This was not investigated further as protein partitioning rather than phase separation behavior was the focus of this study. Values derived by microscopic scoring for observable phase separation at 40× magnification of at least 35 vesicles per condition stained with rhPE.

**Table S1. Quantifications of raft phase partition coefficients ($K_{p,raft}$) of markers and proteins**

| | $K_{p,raft}$ | |
|---|---|---|
| | pdGPMVs | nGPMVs |
| rhPE | <0.1* | <0.1* |
| CTxB | 4.26 ± 0.47 | 3.54 ± 0.45 |
| GPI-GFP | 3.47 ± 1.39 | 3.31 ± 0.95 |
| TfR | 0.23 ± 0.09 | 0.26 ± 0.14 |
| H-Ras | 0.15 ± 0.04 | 0.24 ± 0.06 |
| trLAT | 0.98 ± 0.06 | 1.69 ± 0.23 |
| trLAT-C29A | 0.99 ± 0.06 | 1.17 ± 0.17 |
| trLAT-C26A | 0.51 ± 0.17 | 0.44 ± 0.19 |
| trLAT-IDER dimerized | 0.96 ± 0.14 | 2.64 ± 1.25 |

*Very dim raft phase fluorescence prevents accurate quantification. Shading denotes raft phase enrichment